Composites: Part A 190 (2025) 108626

Contents lists available at ScienceDirect

Composites Part A

journal homepage: www.elsevier.com/locate/compositesa

Demanufacturing of thermoplastic composites: Small scale experiments exploring ply separation and recovery

Andrew J. Parsons [a,*], Michael S. Johnson [a], Samanta Piano [b], Davide S.A. De Focatiis [a]

[a] Composites Research Group, Faculty of Engineering, University of Nottingham, Nottingham, UK
[b] Manufacturing Metrology Team, Faculty of Engineering, University of Nottingham, Nottingham, UK

HIGHLIGHTS

- 12 mm wide PA6, PP and PBT tape plies were peeled apart under controlled conditions.
- The PP and PBT tapes peeled readily at room temperature, PA6 did not.
- The required peel force for PA6 tape ranged from 20 N at 192 °C to 0.26 N at 212 °C.
- Failure mode and resulting surface character was dependent on peel temperature.
- A potential window for PA6 peel without transverse failure is from 200 °C to 215 °C.

GRAPHICAL ABSTRACT

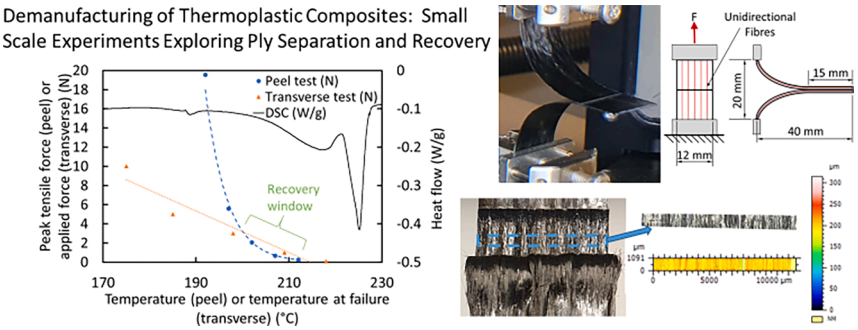

ARTICLE INFO

Keywords:
Thermoplastic resin
Recycling
Tape
Demanufacturing

ABSTRACT

Thermoplastic composites are intrinsically suited to recycling, but processes are poorly realised. Methods applied to thermosets are energy intensive, resulting in fibre downgrading and matrix loss. With digital manufacturing and data intertwining, the exact construction of a component can now be known. As such, instead of destructive recycling, a thermoplastic component might instead be demanufactured by peeling layers apart.

In this study, the potential for recovering thermoplastic tapes by controlled peel was explored through novel small-scale tests. Unidirectional composites of three different tapes (PP/glass, PBT/glass and PA6/carbon) were compression moulded and subjected to transverse, lap shear and peel testing.

Representative load and temperature conditions were established and their effects on the morphology of the recovered tape were considered. It was determined that peeling could be achieved well below the matrix melt temperature with only modest loading, and that contact failure changed from adhesive to cohesive at higher temperatures.

1. Introduction

Thermoplastic composites are experiencing a growth in use in a range of sectors, most notably aerospace and increasingly in the wind industry [1]. As well as offering the same lightweighting potential of thermoset composites, they provide additional benefits such as: higher

* Corresponding author.
E-mail address: andrew.parsons@nottingham.ac.uk (A.J. Parsons).

https://doi.org/10.1016/j.compositesa.2024.108626
Received 4 November 2024; Accepted 26 November 2024
Available online 28 November 2024

operating temperatures; chemical resistance; improved toughness; reduced VOC emissions; precursor storage stability; rapid processing; the ability to be welded [2] and post-forming ability. The development of thermoplastic tapes in particular has enabled very high rate, automated manufacturing [3,4].

With the expected expansion in the use of thermoplastic tapes, there is a pressing need to provide a sustainable lifecycle, especially since the majority of composite precursor materials are still currently oil derived. While there are more sustainable raw materials in development [5,6], the energy costs of producing materials for composites [7,8], in particular carbon fibre, mean that recycling and re-use is essential. There is also socio-political pressure to recycle, with a number of countries already banning landfill or incineration of composites waste [9] and introducing mandates on recycling [10].

However, despite thermoplastic composites being touted as recyclable materials, the actual means of doing so remains relatively poorly realised. The most recent comprehensive reviews on composites recycling [11–18] identified three main existing approaches: shredding, pyrolysis and solvolysis (solvent-based removal). With high value continuous fibre thermoplastics all these methods result in either a downgrading of fibres, a loss of matrix material, or environmental issues and limitations with solvent solubility. The processes are also multi-stage and energy intensive, with a need for downstream processing in order to produce something re-useable from the recovered material [19–21].

A better approach might be to make use of the *thermoplastic* nature of such materials in recycling as is already exploited in manufacturing; the ability to use heat to melt and re-solidify offers the same unique opportunities for debonding and direct recovery. With appropriate control and conditions, composite components could be deconstructed. This would preserve the fibre lengths and maintain intimate contact between fibres and matrix, with minimal matrix degradation and avoiding fibre surface exposure. There are some emerging techniques specific to thermoplastics, such as the bulk moulding compound (BMC)-style moulding of composite chips developed at the ThermoPlastic composites Research Center (TPRC) [22] and the flattening of end-of-life parts to form sheets for subsequent reuse as shown by Kiss et al. [23]. However, challenges remain: in the former, fibre lengths are generally reduced, and in the latter, care must be taken to ensure that fibre directions are preserved and that tow slip and buckling are avoided.

With the advent of manufacturing 4.0, digital ply design and the new paradigm of digital intertwining for manufactured components [8], it is now possible to know the exact construction of a composite component. With this information, the disassembly of the component at end of life ought to be possible [24], avoiding the need to shred it for more energy-intensive and less valuable recycling. For a component produced from thermoplastic composite tapes, the location of each of the tapes is known precisely, making it possible, with suitable confirming metrology systems, to locate the ends of a particular tape. By freeing the end of a tape using a suitable tool and gripping it with the appropriate application of local heat and load, the tape laying process could be reversed – removing the tape and re-spooling it. In such a way the material could be recovered without reducing the fibre length. In order to realise this process, it is necessary to understand the operating window for successful deconsolidation and to begin to explore whether the recovered material is suitable for re-use.

This approach is still quite new, with one of the earliest explorations of this method being used in additive manufacturing to deconsolidate and recover thin tows of poly lactic acid (PLA) impregnated carbon fibre [25]. In that study, by running the molten material through a consolidation die, it was observed that the recovery process actually enhanced the level of tow impregnation. However, some matrix was lost through squeeze out, and the relatively high temperature above the melt caused some molecular weight degradation in the PLA. Several studies have been published by the Fraunhofer institutes on ply-level materials, exploring the recovery of polypropylene (PP), polyamide (PA) and Polyphenylene sulphide (PPS) tapes using ambient or low temperature wedge driven separation [26,27] and peel processes [28,29]. Ultrasonics-assisted peel has also been considered [30], as well as the modelling of the peel process using an analytical method [31].

It is apparent that there is potential in the peel recovery process, though there is a need to better understand the relationship between temperature and required forces, as well as the effects peel recovery has on the resulting recovered material. The previous studies suggest that a low temperature better conserves fibre orientation, whereas a higher temperature potentially provides a better conformation with the peeling process, to provide easier process control and avoid kinking of fibres. Ultimately this information could be applied to an existing tape laying head system with roller and heat source, using the same system to both apply and remove tape–making the peel process perhaps more directly applicable than the wedge method. With a clearer enough understanding, not only is recovery and re-use possible, but on-the-fly corrections could be undertaken during the original part layup with minimum disruption to the fibre architecture.

In this study, the potential for recovery of unidirectionally reinforced (UD) thermoplastic tapes by controlled peel was explored through novel small-scale tests, exploiting the small, heated chamber and axial motion of a rheometer to provide precise control of the process conditions. By undertaking transverse, lap shear and miniature peel tests it was possible to clarify the separate behaviours of the matrix and of combined fibre/matrix interactions. Since the fibre strength and modulus values are significantly higher than those of the polymer, the transverse and lap shear tests provide matrix dominated behaviour. The transverse test affords essentially a 1D contact line failure, while the lap shear provides a 2D areal failure condition. The peel test is representative of the recovery process and includes the effects of fibres loaded in bending. Representative conditions of load and temperature to achieve peeling were established and the effect of these conditions on the morphology of the recovered tape was investigated. Thermoplastic tapes composed of three different polymers were investigated, to compare their behaviour and whether the peel can be used as a general, materials agnostic, method. This work, together with forthcoming studies on larger scale peeling and re-consolidation assessment, forms part of a wider effort towards achieving complete circularity in the manufacturing and demanufacturing of thermoplastic composites.

2. Materials and methods

2.1. Materials

Three distinct unidirectionally reinforced thermoplastic tapes were utilised in this study: polyamide 6 (PA6)/carbon fibre (SGL Group, 45 % V_f carbon, supplied as 400 mm wide tape and cut to 170 mm wide for moulding), polypropylene (PP)/Glass (Comfil, 75 wt% glass, supplied as 50 mm wide tape and used as received) and Polybutylene terephthalate (PBT)/Glass (Comfil, 67 wt% glass, supplied as 50 mm wide tape and used as received). All three polymer matrices are semi-crystalline. These specific materials were selected in order to identify possible differences in behaviour arising from the polymer matrix, the fibres and the volume fraction. PTFE coated glass fabric (Cytec, FF03) was used as a release film in moulding, while aluminium foil (Multifoil, 0.15 mm thick) was used as a shim material.

2.2. Sample moulding

Two-ply UD laminates were produced by compression moulding approximately 220 mm long pieces of tape between rigid flat steel plates. The reinforced tapes were dried overnight in a vacuum oven (Medline scientific OV-11) at 50 °C before moulding and subsequently test samples were similarly dried before testing, to standardise the effect of humidity. Large pieces of tape were used to help balance pressure across the press platen during moulding and to minimise edge effects.

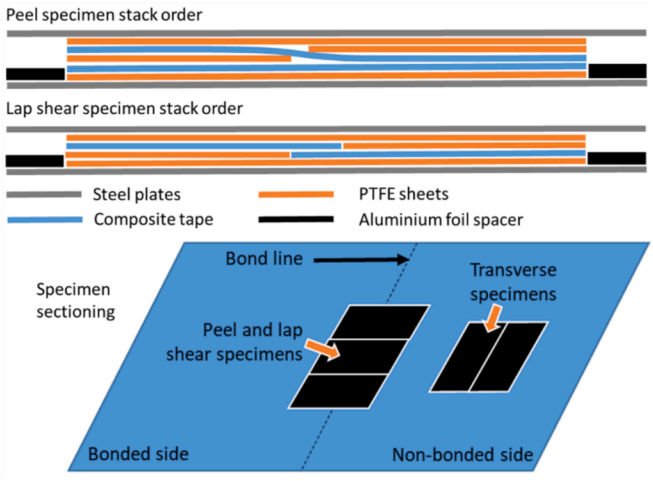

Fig. 1. Schematics showing the stack order when pressing peel and lap shear specimens, along with an indication of the positions from which samples were cut from the larger sheets.

Table 1
Heating rates used for reinforced tapes in DSC and mechanical tests.

Polymer	Ramp 10 °C/min	Ramp 5 °C/min
PP	25–120 °C	120–190 °C
PBT	25–140 °C	140–230 °C
PA6	25–140 °C	140–230 °C

Pieces of PTFE coated fabric were used between plies to create pre-separated ends for peel specimens and as spacers to produce lap shear specimens. Stacks of aluminium foil were used to maintain a minimum separation between the steel plates during pressing.

Assembled stacks of material and plates were introduced to the press at specific temperatures; PP–190 °C, PA6–225 °C, PBT–230 °C, and the platens were closed to firm contact for 10 mins to allow time to melt. An initial pressure of 20 bar was applied, which was then removed and re-applied three times as breathe cycles, before finally holding at 20 bar for a further 10 min. Cooling (on the order of 7 °C/min) was then applied and the samples were demoulded once the temperature was below 50 °C. Nominal thickness of the 2-ply specimens was ~0.4 mm for the PA6/carbon and ~0.5 mm for the PP/glass and PBT/glass.

Test specimens (12 mm wide) were cut from close to the centre of the panels, to ensure the most well aligned fibres. Transverse samples were cut from the separated section of the peel specimens. Schematics of the press stack order arrangements for the Peel and lap shear specimens are provided in Fig. 1, along with an indication of the positions from which samples were cut from the larger sheets.

2.3. Thermal analysis

Materials were characterised using a TA Instruments DSC2500 differential scanning calorimeter (DSC) operating under nitrogen. The DSC was utilised to obtain crystallisation and melting temperature information for the matrix polymers. Heating rates for the DSC are provided in Table 1.

2.4. Mechanical testing

A series of different mechanical tests were performed on the specimens, and these tests are described in this section. A summary of mechanical tests that were performed on each material is provided in Table 2. Photographs and schematics of the test configurations used for these tests are provided in Fig. 2.

2.4.1. Ambient transverse testing

The purpose of the transverse test is to obtain a quantitative measure of the strength of the thermoplastic itself. This is carried out first at ambient conditions in 2.4.1 at fixed rate for comparison, and in 2.4.2 at constant force during a temperature ramp to explore its temperature dependence. Ambient temperature transverse strength tests were carried out for specimens after moulding using a controlled displacement rate at a temperature of 25 ± 1 °C. In each test, a 12 mm wide piece of tape cut in the transverse direction was loaded into the solid rectangular fixture of a rheometer (Anton Paar MCR302) with a grip separation of 20 mm (see Fig. 2(a)). A displacement rate of 25 mm/min was then applied until failure. Multiple (7+) samples were tested for each polymer type. The rheometer allowed for a highly resolved dynamic control of normal force. Failure stress was calculated by dividing the maximum measured force by the product of the width and thickness of the specimen, as determined using a micrometer.

2.4.2. Heated transverse testing

A transverse softening point for each of the as-received tapes was also determined, by using a transverse test temperature sweep under a fixed load, as follows. A 12 mm wide piece of tape cut in the transverse direction was loaded into the grips with a grip separation of 20 mm (see Fig. 2(a)). Temperature ramps were used as listed in Table 1, with an initial rate of 10 °C/min before slowing to 5 °C to match the DSC. The applied load was varied from 0.1 N to 10 N for PA6 and maintained at 0.1 N for the PP and PBT samples. Three different specimens were tested for each type of tape at 0.1 N to determine repeatability. As the results were highly repeatable for the PA6 (difference in onset point between specimens <2 °C), only single specimens were tested at each of the higher loads, in order to obtain more load data. Testing was stopped after a significant increase in sample length was detected, indicating transverse failure.

Table 2
Summary of mechanical tests.

Test performed	PP tape	PBT tape	PA6 tape
2.4.1 Ambient transverse failure	Constant displacement rate 25 mm/min	Constant displacement rate 25 mm/min	Constant displacement rate 25 mm/min
2.4.2 Heated transverse failure	Temperature sweep at fixed 0.1 N load	Temperature sweep at fixed 0.1 N load	Temperature sweeps at fixed 0.1–10 N load
2.4.3 Heated lap shear	Temperature sweep at fixed 1 N load	Temperature sweep at fixed 1 N load	Temperature sweeps at fixed 0.1–10 N load
2.4.4 Ambient peel	Constant displacement rate 25 mm/min	Constant displacement rate 25 mm/min	n/a
2.4.5 Heated peel (fixed load)	Temperature sweep at fixed 0.1 N load	Temperature sweep at fixed 0.1 N load	Temperature sweep at fixed 0.1 N load
2.4.5 Heated peel (set temperature)	n/a	n/a	25 mm/min displacement applied at set temperatures of heating ramp (192 °C, 197 °C, 202 °C, 207 °C and 212 °C

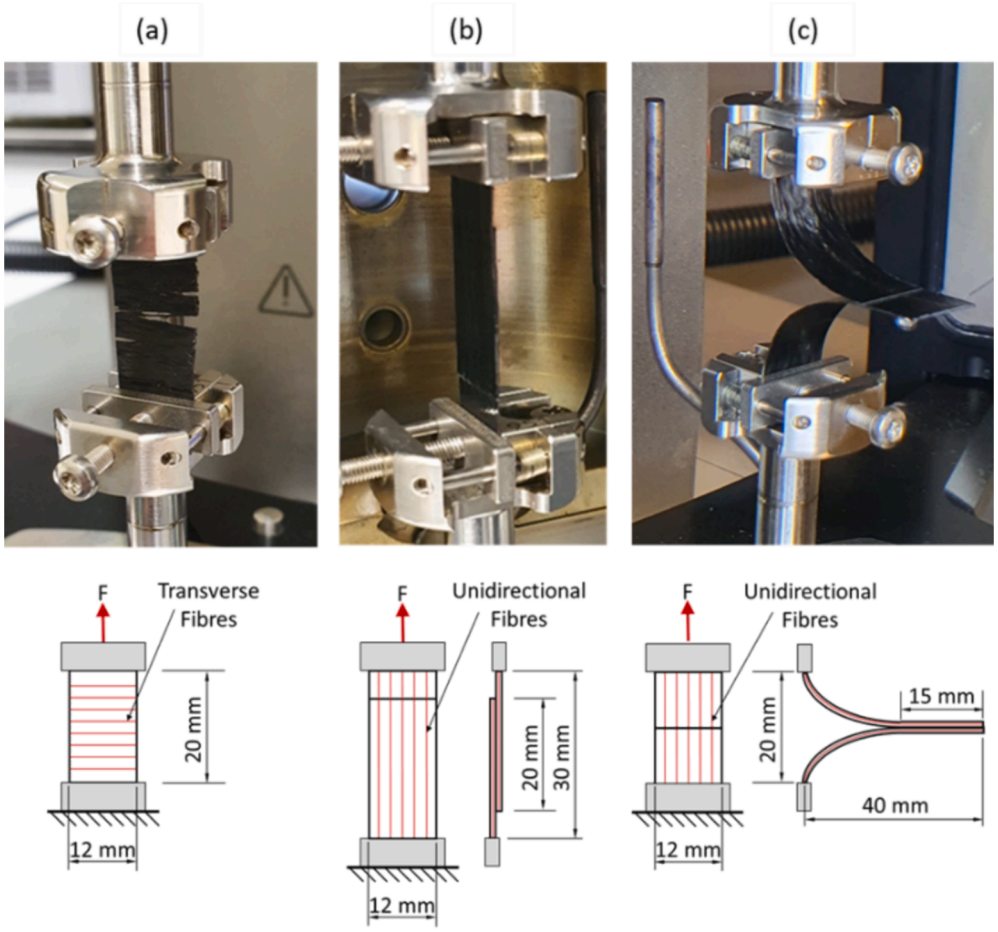

Fig. 2. Photographs and schematics of the test configurations used in the rheometer: (a) Transverse; (b) Lap shear; (c) Peel. In the schematics, the fibre directions are denoted by red lines.

2.4.3. *Heated lap shear testing*

Small lap shear tests were carried out in order to obtain indicative softening points in shear as a comparison to those obtained in transverse extension. The advantage of the shear tests relative to the transverse extension tests is the better defined area across which the shear force is applied, although it is acknowledged that from the point of view of the relevance of the mode of deformation they may be less applicable to a peel scenario. A shear softening point for each of the moulded tapes was determined by using a lap shear-type specimen subjected to a temperature sweep under a fixed load. A 12 mm wide lap shear specimen with a 20 mm overlap was loaded into the solid rectangular fixture of a rheometer with a grip separation of 30 mm (see Fig. 2(b)). Temperature ramps were used as listed in Table 1, with an initial rate of 10 °C/min before slowing to 5 °C to match the DSC. The applied load was varied from 0.1 N to 10 N (in separate tests) for PA6 and maintained at 1 N for the PP and PBT samples. Only two specimens were tested each for PP and PBT at 1 N as they demonstrated nearly identical results. Four samples were tested for PA6 at 1 N, showing good repeatability (<2 °C differences in onset), with single samples tested at other temperatures. Testing was stopped after a significant increase in sample length was detected, indicating shear failure had occurred.

2.4.4. *Ambient peel testing*

The peel characteristics of PP and PBT tape were considered through a miniature peel test at an ambient temperature of 23 ± 2 °C. A 12 mm wide specimen with 15 mm bonded length and a total length of >40 mm was loaded into the grips with a 20 mm grip separation in a T-peel configuration (see Fig. 2(c)). The grips were displaced at 25 mm/min and the peeling (normal tensile) load recorded. Due to the geometric constraints, the force recorded during this initial displacement included a component that was due to the curvature of the fibres. Since the curvature of the fibres changes with displacement, so does this force. In order to isolate the peel force from this bending force, a further experimental step was necessary. After the initial peel, the grips were returned to their initial displacement without removing the sample. This returned

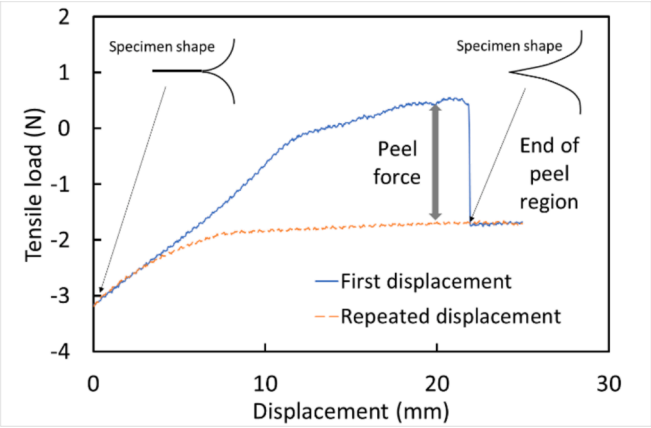

Fig. 3. Example of the baseline correction used for peel. During the first displacement, the sample is peeled. In the repeated displacement the forces incurred by the sample shape remain, but the bond is no longer present. The peel force is determined as the difference between the two load curves.

the fibres to the same curvature as at the start of the test, but without any bond between the plies. By then repeating the displacement without the bond, only the force due to fibre curvature as a function of displacement was measured. This value was then subtracted from the initial force displacement data in order to provide a measurement of the peel force (see Fig. 3). Due to the confined space, it was extremely difficult to load the specimens without damage, more so with the PP than the PBT. As a result, only 4 satisfactory tests could be performed with PP and 6 with PBT.

Ambient peeling was not possible with the PA6 specimens as the required load exceeded the load cell capability of the rheometer (40 N).

2.4.5. Heated peel testing

The peel characteristics of the PA6 tape were considered through a heated miniature peel test. A 12 mm wide specimen with 15 mm bonded length and a total length of 40 mm was loaded into the grips with a 20 mm grip separation in a T-peel configuration. Initially, a temperature ramp was applied as listed in Table 1 with a fixed tensile load of 0.1 N. This resulted in an inconsistent behaviour, likely due to relaxation of the peel sample on heating. Instead, a heat-cool-heat cycle was applied. In the initial heat and cool process, the sample was held at a fixed position to allow relaxation to occur. In the second heating cycle the fixed tensile load of 0.1 N was then applied and the consistency of the result was satisfactory (<2 °C difference in onset) across triplicate samples.

Subsequently, to investigate the effect of peeling load, the samples were again heated at a fixed position before being subjected to a rapid peeling displacement (25 mm/min) at five different temperatures near the melting point: 192 °C, 197 °C, 202 °C, 207 °C and 212 °C. Load values were recorded for each temperature as a function of displacement.

Similar testing was not applied to the PP and PBT tapes as they were observed to begin peeling at ambient temperature when applying the 0.1 N fixed load.

2.5. Optical characterisation

2.5.1. Crack tip

Post manufacturing, representative specimens of the bonded section were excised for each polymer type and potted in clear epoxy resin (PC15 Water Clear Polyurethane 2-part casting resin, Easy Composites). These were then polished sequentially under flowing water with wet-and-dry abrasive paper in a Struers LaboPol-30 with LaboForce-50, followed by finishing with 1 μm diamond paste. The bonded region and crack tip were then imaged on an Olympus BX51 microscope equipped with an Infinity 2 digital camera using dark field reflected light illumination and lenses. The images were focus-stacked using the Fiji extended depth of field plugin.

2.5.2. Peeled surface

Surface assessment was undertaken for the PA6 peel test specimens that were subjected to a delayed peeling load at five different temperatures as described in section 2.6.2. The surfaces of ~10 mm × 1.5 mm regions of the samples were measured using an Alicona G5 focus variation metrology system using a 20x lens to generate a point cloud data set. This data was then processed by using Mountains software, applying ISO 25178 to generate cross sectional height graphs to show the height change in several positions along the samples. Surface roughness (S_a) and related root mean square (S_q) values were also determined.

Table 3
Ambient transverse stress at failure (MPa).

Polymer	Failure stress (MPa)	*n*
PP	0.2 ± 0.1	7
PBT	0.3 ± 0.1	7
PA6	9.0 ± 3.0	8

3. Results

3.1. Mechanical test results

3.1.1. Ambient transverse tests

The ambient temperature transverse failure stresses are presented in Table 3 for the three tapes. Stresses at failure in transverse testing at room temperature were small and PP and PBT specimens were notably fragile during loading. Although there is variability, it is apparent that the PA6 tape has a substantially higher ambient transverse strength than the PP and PBT tapes.

3.1.2. Heated transverse tests

The displacement vs temperature results at fixed load for the heated transverse tests are provided in Figs. 4–6. DSC information is superimposed on the results. For PBT and PA6, loaded by 0.1 N, the apparent softening point correlated well with the peak of the initial melting endotherm. For PP, the softening point appeared to occur as much as 30 °C lower than the endotherm peak. For the PA6, increasing the load reduced the failure temperature significantly, from approximately 218 °C at 0.1 N to 175 °C at 10 N. Additional loads were not applied to the PP and PBT tape due to their low failure loads at ambient conditions.

3.1.3. Lap shear test results

The lap shear displacement vs temperature measurements at constant load are provided in Figs. 7–9. When tested at 1 N, the shear softening point correlated well with the dominant endotherm of the PA6 and PBT samples, and with the single endotherm for PP. A load of 0.1 N was insufficient to cause shearing, but the replicates at 1 N indicated good consistency. Increasing the load for the PA6 up to 20 N resulted in a shear failure at reduced temperature, by as much as 7 °C (from ~223 °C at 1 N to 216 °C at 20 N). This is still within the melting region identified by DSC and is a much smaller effect of load than was observed for transverse loading. The lower load specimens experienced good axial displacement, with the long overlap providing resistance to the bending moment than can be observed in standard lap shear testing [32]. However, there was a small amount of necking through out of plane wrinkling, see Fig. 10. This necking and deformation increased at higher displacements due to the force-controlled nature of the test.

3.1.4. Ambient peel tests – PP and PBT

Ambient temperature miniature peel test measurements of load and displacement are provided in Figs. 11 and 12 for PP and PBT tape, respectively. As noted in 2.6.1, it was not possible to perform an ambient peel test with the PA6 due to the load limit of the test system. It is

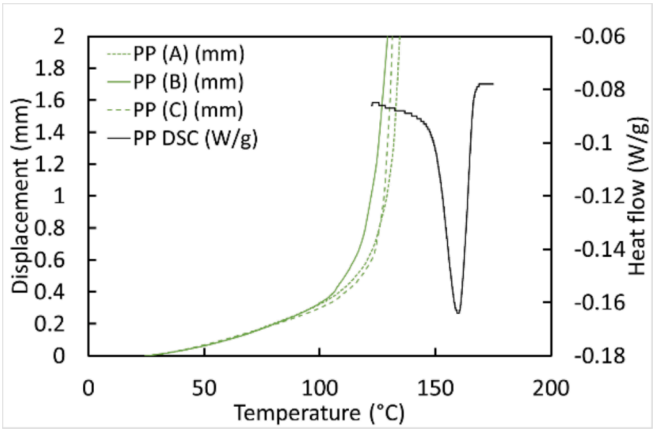

Fig. 4. Displacement measured for replicates A-C during a temperature ramp at constant 0.1 N load on 12 mm wide transverse specimens of thermoplastic PP tape (left ordinate axis); DSC melting endotherm (right ordinate axis).

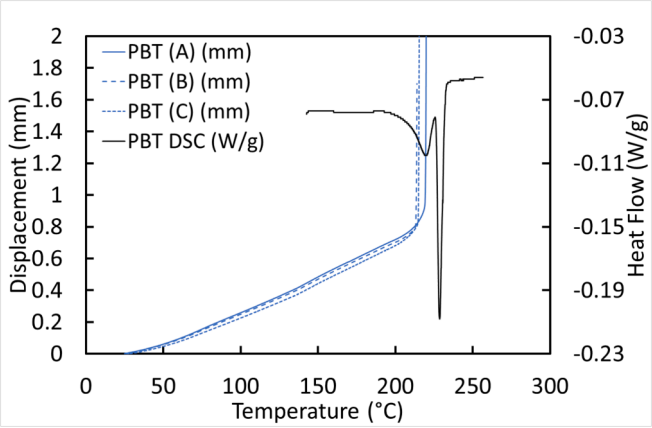

Fig. 5. Displacement measured for replicates A-C during a temperature ramp at constant 0.1 N load on 12 mm wide transverse specimens of thermoplastic PBT tape (left ordinate axis); DSC melting endotherm (right ordinate axis).

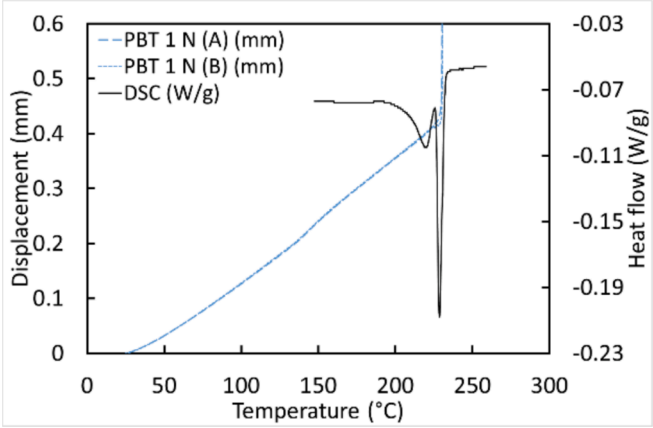

Fig. 8. Displacement measured for replicates A-B during a temperature ramp at constant 1 N load on 12 mm wide lap shear specimens of thermoplastic PBT tape (left ordinate axis); DSC melting endotherm (right ordinate axis).

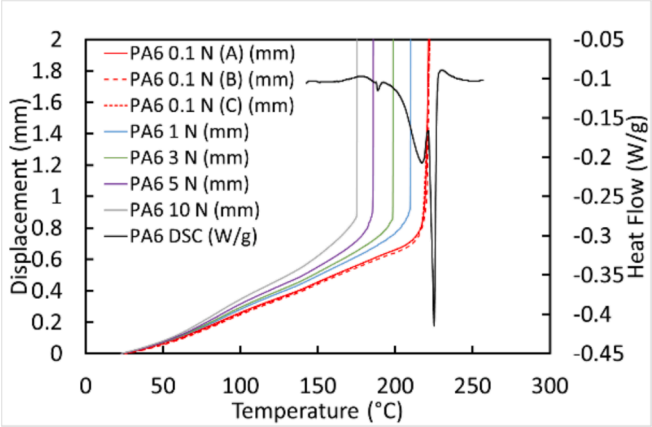

Fig. 6. Displacement measured during a temperature ramp at constant loads (three replicates (A-C) at 0.1 N and one specimen each for 1, 3, 5 and 10 N) on 12 mm wide transverse specimens of thermoplastic PA6 tape (left ordinate axis); DSC melting endotherm (right ordinate axis).

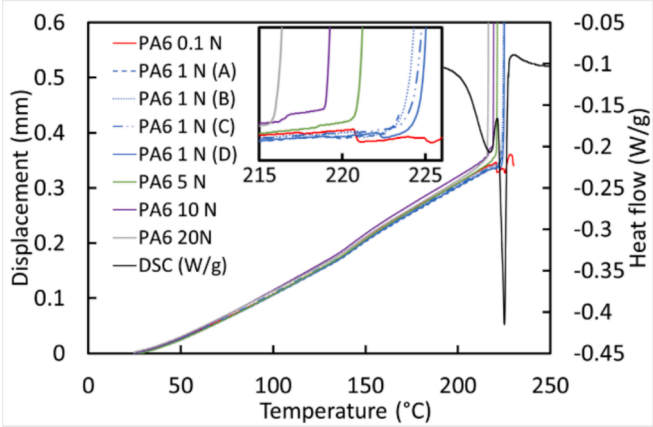

Fig. 9. Displacement measured during a temperature ramp at constant loads (Four replicates (A-D) at 1 N and one specimen each for 0.1, 5, 10 and 20 N) on 12 mm wide lap shear specimens of thermoplastic PA6 tape (left ordinate axis); DSC melting endotherm (right ordinate axis). Inset shows a close up of the displacements in the region of peel onset.

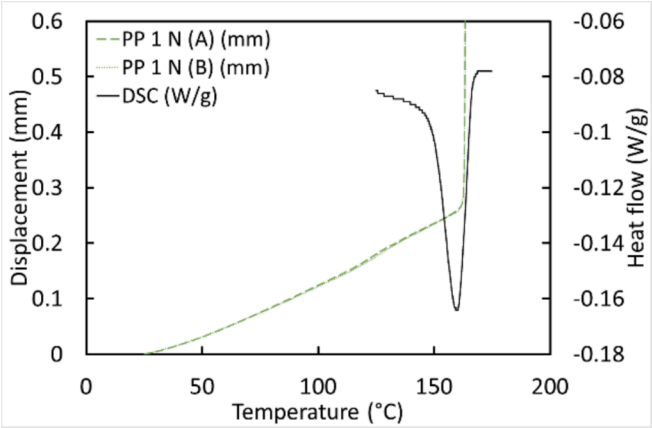

Fig. 7. Displacement measured for replicates A-B during a temperature ramp at constant 1 N load on 12 mm wide lap shear specimens of thermoplastic PP tape (left ordinate axis); DSC melting endotherm (right ordinate axis).

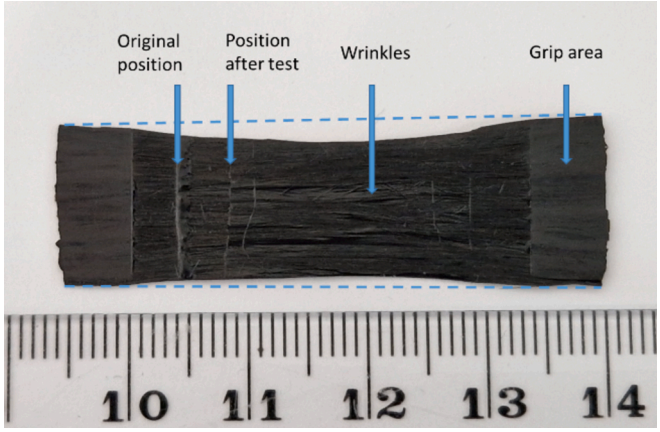

Fig. 10. Photograph of a PA6 lap shear specimen after testing with a temperature ramp at 1 N load, showing deformation.

probable that either the level of crystallinity in the PA6 specimens led to a tougher matrix in the PA6 compared to the PP and PBT, or perhaps that the crack tip at the point of peel may be sharper in the PP and PBT specimens. The force data has been computed by subtracting the force measured in the reload cycle at the same displacement from the force measured during the first (peel) cycle, in order to remove the elastic

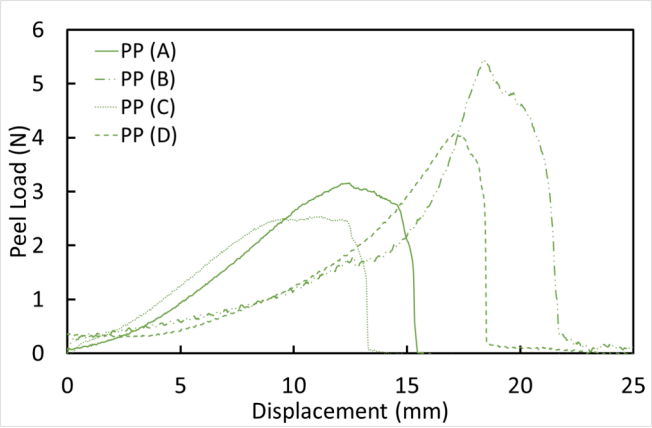

Fig. 11. Replicates A-D of peel force as a function of displacement for 12 mm wide reinforced PP tape specimens peeled at 25 mm/min. The peel force is computed by subtracting the force recorded on a second displacement (after returning to zero displacement) from the force recorded on the first displacement (see section 2.4.4).

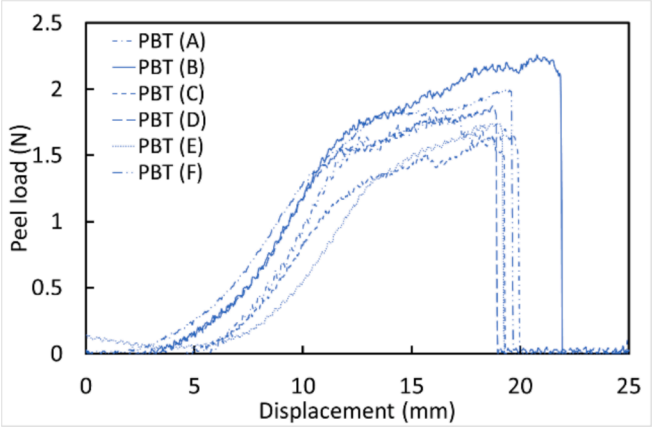

Fig. 12. Replicates A-F of peel force as a function of displacement for 12 mm wide reinforced PBT tape specimens peeled at 25 mm/min. The peel force is computed by subtracting the force recorded on a second displacement (after returning to zero displacement) from the force recorded on the first displacement (see section 2.4.4).

bending effects. The peel load increases with displacement through to a brief plateau in the PBT, and to a less well-defined plateau in the PP, in some cases reaching a maximum and falling quickly afterwards. The PBT provides a more reproducible peel curve than the PP, but both were difficult to load without damage to the fibres due to the tight radius of curvature required for loading.

3.1.5. Heated peel tests – PA6

3.1.5.1. Heat-cool-heat tests. Specimens of PA6 were loaded in a peel configuration with a fixed tensile load of 0.1 N, and the temperature was ramped up according to Table 1. Changes in the material upon heating resulted in rapid but not always reproducible relaxation of stresses, and the feedback loop on the rheometer was unable to act quickly enough to maintain the constant load. This occurred in the region of 150 °C, well below the melt temperature. Examples of this effect are shown in Fig. 13.

An alternative methodology was devised to reduce the effect of the residual stresses that are induced by loading the peel specimens in the grips. Peel samples were loaded, and first heated and cooled at a fixed grip displacement. This results in a residual tensile load on the specimens. The system is switched from displacement control to load control,

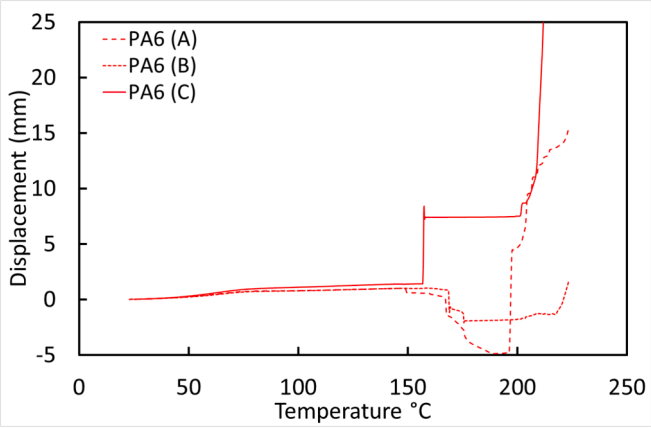

Fig. 13. Replicates of displacement measured during a heating temperature ramp at 0.1 N constant load on 12 mm wide peel specimens of thermoplastic PA6 tape.

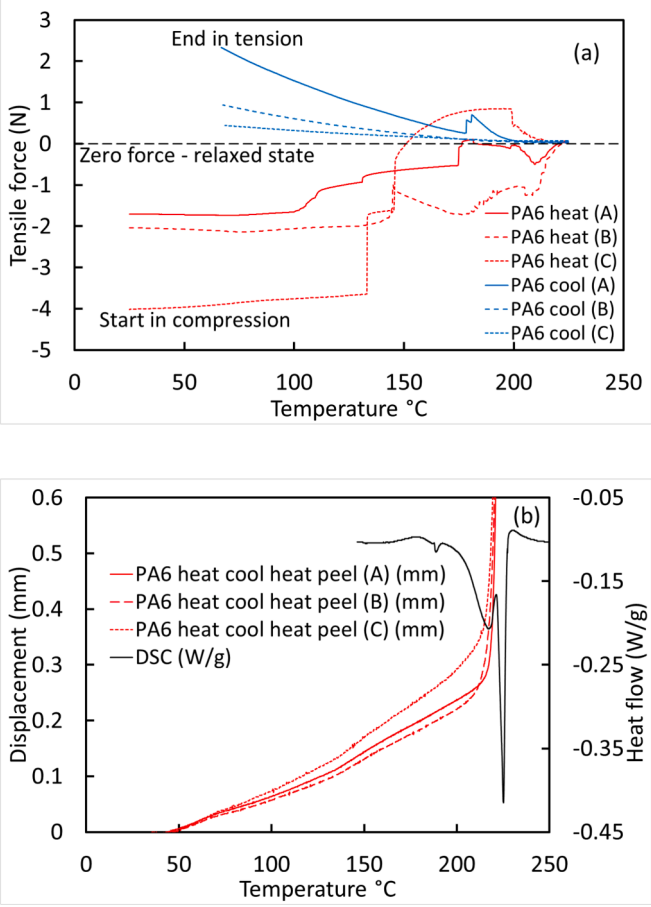

Fig. 14. (a) Replicates A-C of tensile force measured during a heating and cooling temperature ramp at fixed displacement on 12 mm wide peel specimens of thermoplastic PA6 tape. The force starts out as compressive, reaches zero at the highest temperature, then becomes tensile during cooling. (b) Replicates A-C of displacement measured during a temperature ramp at constant 0.1 N force on 12 mm wide peel specimens of thermoplastic PA6 tape following an initial heating and cooling cycle at fixed displacement (left ordinate axis); DSC melting endotherm (right ordinate axis).

and the load is reduced to 0.1 N. This causes the grips to come together to reduce the tensile load. The specimen is then re-heated under a constant 0.1 N tensile load, and the displacement monitored. The first

displacement-controlled heat-cool stage is shown in Fig. 14(a) and the second load-controlled heating in Fig. 14(b).

It can be seen in the first heating process that the load tends to zero as the sample is heated, relaxing the bending stresses. On cooling a contraction force is incurred through shrinkage, since the displacement is fixed, indicating that the sample maintains integrity. On second heating with a fixed load (Fig. 14b) the peel behaviour is well defined, with a similar profile in relation to the DSC that was seen for the transverse tests (Fig. 6).

3.1.5.2. Displacement controlled tests. A different experiment was performed in which the temperature was ramped at a fixed displacement. When temperatures of 192 °C, 197 °C, 202 °C, 207 °C, 212 °C were reached, close to but straddling the melting endotherms, the sample was peeled at a constant rate of 25 mm/min. The raw peel force and displacement are shown in Fig. 15. Relaxation of the initial compressive force is observed as before during the heating, with a distinct tensile force peak when rapid peel is applied. The magnitude of the peak peel force is reduced at higher temperatures.

3.2. Optical characterisation

3.2.1. Crack tip

Cross sections of the crack tip for each of the polymers are provided as microscopy images in Fig. 16. The positioning of the PTFE sheets used to create the non-bonded section are readily apparent in the images. A matrix-rich region can be observed where the fibres have not fully conformed around the PTFE sheets.

3.2.2. Peeled surface

The surface assessments of the PA6 specimens peeled at specific temperatures (as shown in Fig. 15) are provided in Fig. 17. Optical images show qualitative differences, while high-resolution microscope images are provided for each, alongside their waviness contour. Their S_a and S_p values are provided in Table 4, measured across an area of approximately 10 mm × 1.5 mm. The lowest temperature peel (192 °C) appeared to suffer a sub-melt cohesive failure, requiring the highest force to peel but resulting in a relatively smooth peeled surface with no visible surface fibres. The samples at 197 °C and 202 °C, which required less force to peel, exhibited adhesive failure at the fibre surfaces and a relatively rough peeled surface. The highest temperate samples (207 °C and 212 °C) required very little force to peel and appeared to suffer cohesive matrix failure, showing a shiny, melted surface.

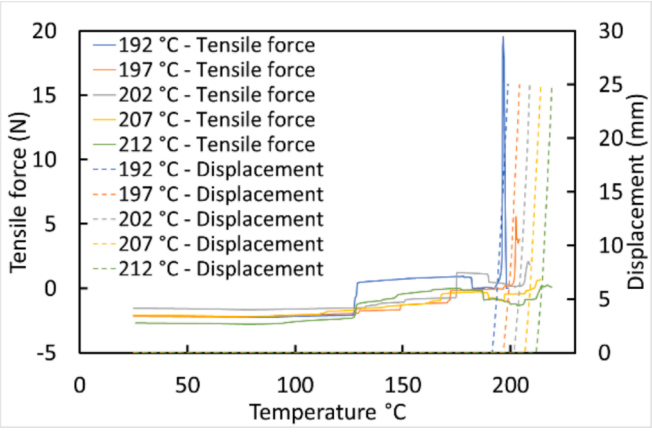

Fig. 15. Replicates of force measurements during a temperature ramp at fixed displacement to 192 °C, 197 °C, 202 °C, 207 °C, 212 °C, followed by peel displacement at a rate of 25 mm/min, on 12 mm wide peel specimens of thermoplastic PA6 (left ordinate axis); displacement is shown on the right ordinate axis.

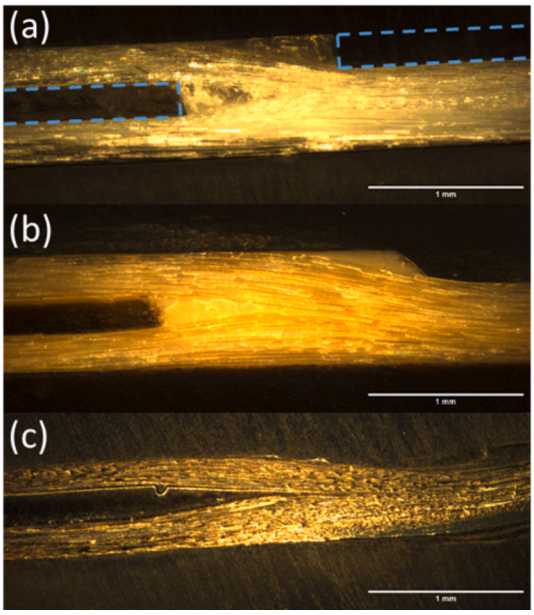

Fig. 16. Darkfield optical micrographs of the crack tip profiles prior to peel testing for each of the three types of tape: (a) PP/glass, (b) PBT/glass and (c) PA6/carbon. The approximate position of the PTFE sheets used to separate one side of the tapes is indicated in image (a) with dashed lines.

4. Discussion

4.1. Mechanical tests

The use of a rheometer to study unidirectionally reinforced thermoplastic tapes enabled very good control of both tensile load and temperature to provide consistent data in the majority of tests. Both the lap shear data and the transverse tests at temperature were very repeatable and consistent (difference in onset point between specimens <2 °C). The force data from the room temperature transverse tests was less reliable, likely due to the low overall loads and fragility of the samples resulting in localised but undetected damage during loading or cutting. Although the peel data was more challenging to obtain, primarily because of the confined space and the small radius of curvature of the initial peel specimen, it appears to be consistent if appropriate experimental protocols are employed.

4.1.1. Transverse and lap shear

Of particular note is the difference in failure temperature between transverse and lap shear specimens. Since the fibre strength and modulus values are significantly higher than those of the polymer, both of these tests are primarily matrix dominated. At low loading, both tests indicated that a degree of crystalline melting is required before failure. However, the transverse tests failed at a temperature corresponding to the early onset of melting (Figs. 4–6) while the lap shear tests only failed once the matrix was almost fully molten (Figs. 7–9). This fits with logical expectation. Since the transverse test applies load to an essentially 1D line of polymer, a weakest link failure occurs. With the lap shear test, an area of polymer is under load and needs to melt across a significant portion of the area for failure to occur. It was also observed that the load applied has a significant effect on the transverse failure (Fig. 6), but only a limited effect on the lap shear failure (Fig. 9). This is again a scaling effect, since the added load would have a much smaller effect on the local stresses in the large overlap area, in comparison to the small area of the transverse test.

In terms of practical application this difference offers potential benefits to process control. The peeling process is relatively similar to the transverse mode, in that peeling is in effect a moving, near-1D line.

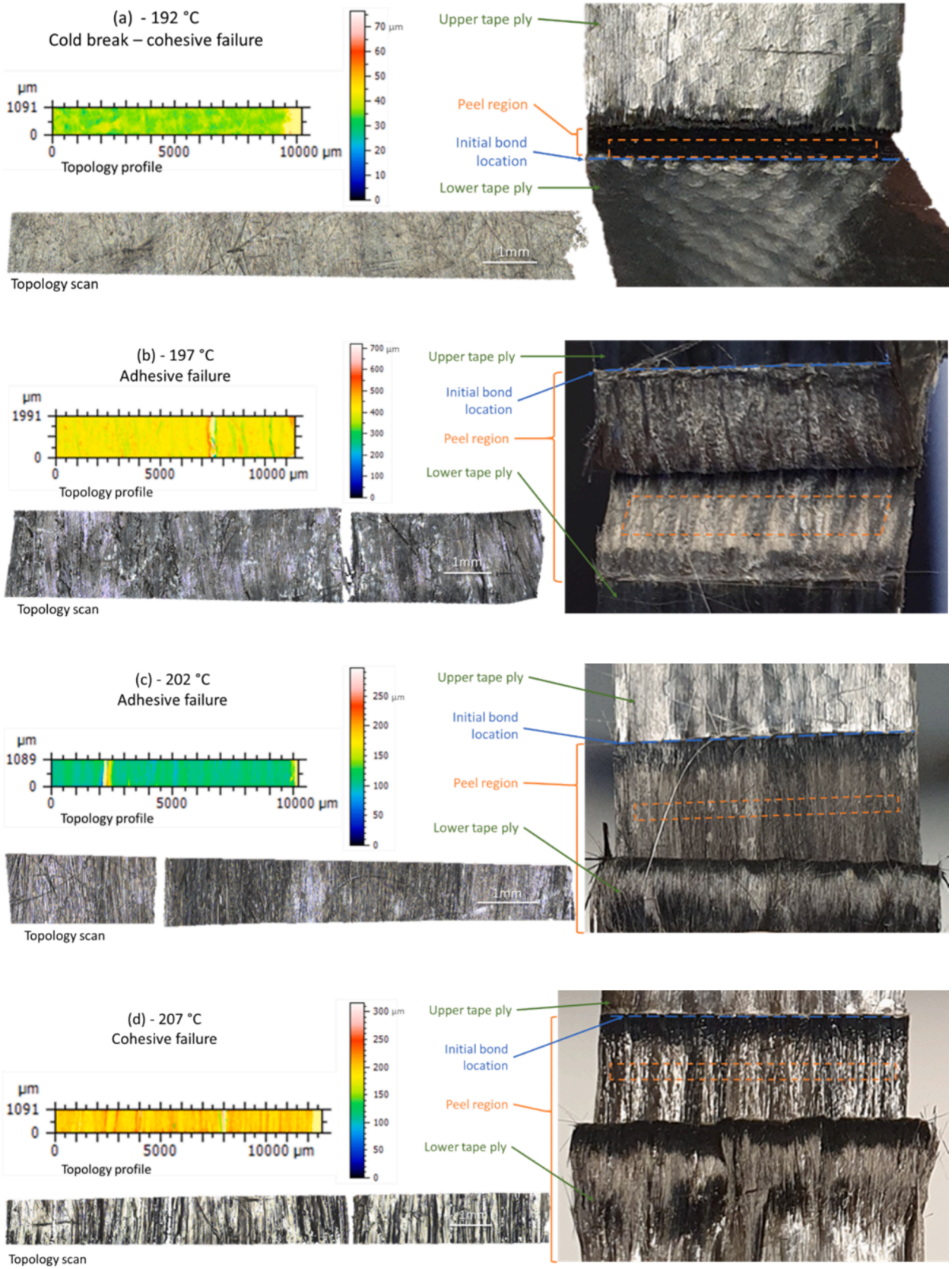

Fig. 17. Optical images of the peeled surfaces of the reinforced PA6 tape peeled at (a) 192 °C; (b) 197 °C; (c) 202 °C; (d) 207 °C and (e) 212 °C; Alicona-derived digital microscope images of a thin section across the width of the tape (approximate location denoted by dashed outline) and contour plots of the surface profile.

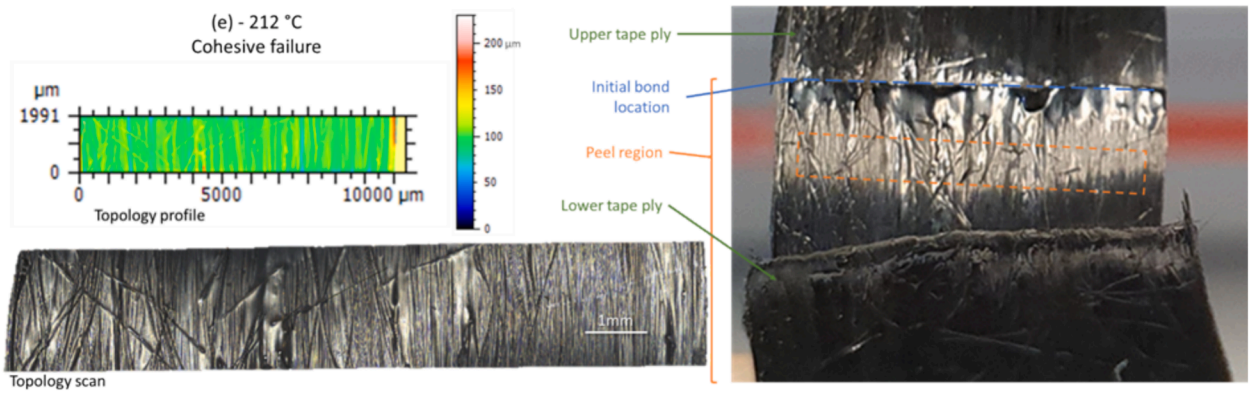

Fig. 17. (*continued*).

Table 4
Surface profile parameters for PA6 specimens peeled at different temperatures. S_a is the surface roughness (arithmetical mean height) across an approximately 10 mm × 1.5 mm area and S_q is the root mean square value.

Peel temperature (°C)	$S_a \pm S_q$ (µm)
192	1.63 ± 2.2
197	15.5 ± 25.3
202	8.58 ± 13.2
207	9.46 ± 14.5
212	7.68 ± 11.3
As received surface	2.67 ± 3.6

The lap shearing mode of areal shift would instead apply in relation to the tape moving from side to side, or other gross slip in-plane (for example, upon reaching the end of a tape). As such, the process window for stable peeling without slip should lie between early onset of crystallisation and full melt and could be determined via DSC for a given matrix. Further, tension driven control could be used to smooth the peeling process in this window without inducing slip.

4.1.2. Peel

A peel test is intended to be the closest representation to a process of demanufacturing and recovery of thermoplastic tapes. In a peel test a small thin region of polymer is separating at any given point, and in this manner it is perhaps closer in nature to the transverse test than to the lap shear test. This is supported by the PA6 peeling behaviour observed in Fig. 14(b), with the peel occurring at a temperature similar to that seen with the transverse test (Fig. 6).

4.1.2.1. Ambient peel (PBT and PP). The successful room temperature peel tests carried out on PP and PBT indicate that these materials would be easily recoverable by peel. The forces required for peeling were surprisingly low (Figs. 11 and 12), even considering that they are applied to a very small area. Other studies on woven PP material do not appear to report the actual forces required to peel, though the manual effort used to peel illustrated in one [28] suggests that they are low.

While both the PBT and PP tapes peeled readily at room temperature at relatively low loads, it was not possible to peel the PA6 tape at room temperature. This may be due to two factors: the state of the crack tip, and the free end of the specimen.

In looking at the crack tip images in Fig. 16, there is a matrix-rich region at the junction between the 2 plies of material as a result of the moulding process. With the PBT and to some extent the PP this excess matrix appears to be cracked, potentially providing a sharp crack tip to easily propagate peel. With the PA6 this matrix-rich region is more difficult to identify due to the presence of carbon rather than glass fibres.

In future studies, there is a need to revisit the nature of the start of the peel process and how the initial delamination is induced to create a crack tip. Several methods have been considered in other studies, including short beam shear, impact (end on and lateral) [28] and ultrasonic knife [30], as well as a pre-installed crack generator such as an expanding component [33]. The most practical approach will likely be both part and cost dependent.

In heated tests the initial state of the crack tip becomes less important since the matrix is transforming into a molten state such that the separation is potentially driven more by viscosity and surface tension.

4.1.2.2. Heat-cool-heat peel (PA6). The unusual behaviour observed in the initial heated peel testing for PA6 (i.e. significant deformation of the material far below the crystalline melting point (Fig. 13) can perhaps be explained through the transverse behaviour. Even with a fixed displacement or very low externally applied load, there is considerable spring loading in the peel specimen due to the small bending radius. While the majority of the load is carried elastically by the fibres, the relative position of the fibres is dependent on the polymer matrix between them. Since PA6 is semi-crystalline, there is a degree of mobility above T_g of the amorphous phase that could enable reconfiguration under load. The 'tail' of the peel specimens was observed to droop during testing and a degree of curvature could occur in the part of the peel specimens yet to be peeled. This suggests a limitation of the rheometer-based approach to investigating peel testing in that it relies on an isothermal environment; for the purpose of tape separation it would be preferable only to heat the immediate peeling region.

Nevertheless, by fixing the displacement of the specimen and taking it to its melt point the spring forces can be relaxed as the specimen adjusts shape to a minimum stress state (Fig. 14a). During cooling a small load is induced, likely due to shrinkage, but this was accounted for by switching to load-control in the second heating. By introducing this heat-cool relaxation of the samples at fixed displacement, it was possible to obtain reproducible peel information (Fig. 14(b)) with the peeling occurring near the onset of crystalline melting for PA6 under a load of 0.1 N.

4.1.2.3. Displacement controlled peel (PA6). The effect of load on transverse failure (Fig. 6) suggested that the peel temperature for the PA6 could be reduced by applying additional load. To investigate this, rather than utilising a force control approach that required the heat-cool heat stabilisation, samples were instead tested under displacement control at a range of temperatures. During heating at constant rate, when a pre-selected selected target temperature was reached, the sample was displaced at a fixed rate and the force monitored. The peak peel load for each of the hot-peeled PA6 specimens from Fig. 15 is approximately an exponential function of the peel temperature. This suggests the possibility of recovery well below the peak melt temperature of the matrix by using modest force. Potentially this might be reduced further

by modification of the initial crack tip formation and by introducing a constraint to prevent curvature and fibre kinking, such as through a peel roller.

4.2. Characterisation of the peeled surface

The temperature and load experienced by the tape during separation has a significant effect on the quality of the recovered tape. Low temperatures, and hence high forces, have been previously observed to result in kinking and fibre tear out [29], whereas high temperatures, whilst reducing the peel forces, can result in matrix degradation [25] as well as surface tension-driven molten matrix redistribution.

The surface metrology results shown in Fig. 17 indicate three regions of separation behaviour for the PA6 tape. There is a region at 207 °C and above (Fig. 17 (d) and (e)) where the matrix is mobile enough to create a cohesive failure, with a characteristic 'shiny' finish. In the 197–202 °C window (Fig. 17 (b) and (c)) there is an apparent fibre adhesive failure, with a characteristic matt finish and evidence of fibre tear out, which could give a resin-starved surface potentially requiring re-processing before re-use. However, at an even lower temperature of 192 °C (Fig. 17 (a)), cohesive failure is observed resulting in a smoother fracture surface with no evidence of exposed fibres, albeit with a higher required separation force. It is possible that fibre kinking may have occurred here, but it is obscured by the matrix.

4.3. Consideration of multi-ply peeling

Overall for peeling, it is enticing that it might be possible to recover tapes at relatively low temperature using modest forces of only a few newtons, essentially intact ready for re-use. Some level of reprocessing may be required to redistribute the matrix and smooth the surface prior to a second manufacturing operation, depending on the particular process. It is worth noting, however, that if recovery of tapes is to take place in a real component at end-of-life, peeling recovery is likely to be from a cross-ply material, which was not considered in this study. In such a situation, the fibres in the layer below the tape being peeled may be at 45° or even 90° to the peeling process. At 90° this would place the lower layer into an essentially transverse failure condition, and mechanical constraints may be required to prevent damage to the lower layer.

By comparing Table 3 and Figs. 11 and 12 it can be seen that the transverse failure load appears to be lower than the peel load for the PP and PBT specimens at ambient conditions (0.7 N vs 2.5–5 N for PP and 1.1 N vs 1.3–2.2 N for PBT). As such, peeling non-woven PP and PBT materials with 0/90 ply configuration may be very difficult as the sub-layer could split.

For the PA6, the transverse failure load under ambient conditions was much greater than for PP or PBT but reduced with temperature. In Fig. 18, the transverse failure loads obtained for PA6 from Fig. 6 are plotted alongside the peel loads from Fig. 15.

There is a short window between approximately 200 °C and 215 °C in which the peel forces are lower than the forces at which transverse failure occurs at the same temperature. This offers the potential for successful peel. It is worth noting that for the widths of tape tested here the absolute force values are small, and so this may be challenging to control with narrow tapes.

The situation in a multi-directional lay-up is more complex, however it is also possible that a carefully controlled non-isothermal peel could selectively weaken the specific bond area intended to peel. The anisotropy of the thermal conductivity due to the presence of unidirectional fibres in different orientations could also be exploited for peel process control. Thermal energy will diffuse more easily along the more thermally conductive fibre directions than the more thermally insulating layers of polymer [34–36].

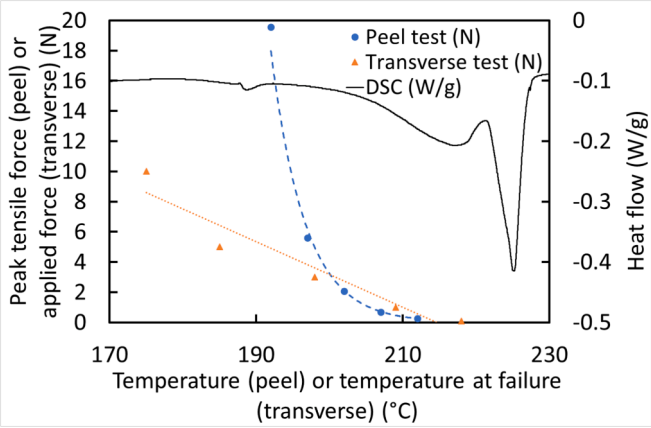

Fig. 18. Peak force vs temperature for reinforced PA6 tape with transverse loading and with fixed displacement and delayed peel. DSC data is shown to indicate onset of melting. Measurements of peak tensile force during peel following a temperature ramp at fixed displacement to 192 °C, 197 °C, 202 °C, 207 °C, 212 °C, and of the temperatures of failure during transverse specimen temperature ramps loaded at varying force (left ordinate axis); DSC melting endotherm (right ordinate axis).

5. Conclusions

This study has employed miniature experiments to investigate the demanufacturing of three types of thermoplastic tapes. A rheometer with environmental chamber was used effectively in determining transverse and lap shear properties of thin laminates. It was also used for a preliminary investigation of peel geometries.

It was observed that, in general and for a similar applied global load range (0.1–20 N), matrix failure as witnessed by transverse tests occurs at temperatures at or below the melting endotherm, while lap shear failure only occurs at higher temperatures. Although it was not possible to reproduce the same experiments in peel geometries, it was possible to measure the peak peel force at specific test temperatures across the melting endotherm.

The results obtained indicate that disassembly of components made using UD thermoplastic tapes is eminently feasible, can be performed below peak melting temperatures and requires relatively small peel forces. The resulting morphology of the fibre surface is dependent on the temperature used, with different failure modes observed at different temperatures. The PP and PBT tapes peeled readily at room temperature, while the PA6 tape required an elevated temperature. The force required to peel the PA6 tape was reduced with increasing temperature, from 20 N at 192 °C to 0.26 N at 212 °C.

The high load peel at 192 °C appeared to cause a cohesive failure with a resulting smooth surface. Between 197 °C and 202 °C the failure became adhesive with evidence of dry fibres. At 207 °C and above the failure became cohesive again, with evidence of matrix flow resulting in a rougher surface but without dry fibres.

A simple comparison of transverse and peel forces suggests that cross ply peeling may be feasible in specific temperature windows where the peel force is less than the transverse failure load (between 200 °C and 215 °C for PA6 in this case), but more work is required to consider this specific aspect. Work is on-going in our laboratory to explore localised heating at the peel front at a more representative length scale, in order to investigate a continuous peeling method that would be required for practical demanufacturing.

CRediT authorship contribution statement

Andrew J. Parsons: Conceptualization, Data curation, Formal analysis, Investigation, Methodology, Visualization, Writing – original draft, Writing – review & editing. **Michael S. Johnson:** Methodology,

Writing – review & editing. **Samanta Piano:** Methodology, Resources, Supervision, Writing – review & editing. **Davide S.A. De Focatiis:** Conceptualization, Funding acquisition, Methodology, Project administration, Resources, Supervision, Visualization, Writing – review & editing.

Declaration of competing interest

The authors declare that they have no known competing financial interests or personal relationships that could have appeared to influence the work reported in this paper.

Acknowledgements

This work was funded by the Engineering and Physical Sciences Research Council through the Future Composites Manufacturing Research Hub Feasibility Grants program (Grant number: EP/P006701/1). The authors would like to acknowledge Nathan Roberts of the Manufacturing Metrology Team in the acquisition of metrology data using the Alicona system.

Data availability

Data for this paper will be hosted in Mendeley Data and can be found here DOI: 10.17632/pwdx6hxcv9.1

References

[1] Market Research Future report ID: MRFR/CnM/2891-HCR. Thermoplastic Composites Market. 2022. https://www.marketresearchfuture.com/reports/thermoplastic-composites-market-4244, accessed 01.07.24.
[2] Worrall C, Kellar E, Vacogne C. Joining Of Fibre-Reinforced Polymer Composites. accessed 01.07.24 A Good Practice Guide 2020. https://compositesuk.co.uk/wp-content/uploads/2021/12/Joining-Good-Practice-Guide-FINAL.pdf,.
[3] Donough MJ, Shafaq, St John NA, Philips AW, Gangadhara Prusty B. Process modelling of In-situ consolidated thermoplastic composite by automated fibre placement – A review. Composites Part A: Applied Science and Manufacturing. 2022;163:107179. https://doi.org/10.1016/j.compositesa.2022.107179.
[4] Yassin K, Hojjati M. Processing of thermoplastic matrix composites through automated fiber placement and tape laying methods:A review. J Thermoplast Compos Mater 2018;31(12):1676–725. https://doi.org/10.1177/0892705717738305.
[5] Wang S, Bai J, Innocent MT, Wang Q, Xiang H, Tang J, et al. Lignin-based carbon fibers: Formation, modification and potential applications. Green Energy Environ 2022;7(4):578–605. https://doi.org/10.1016/j.gee.2021.04.006.
[6] Newcomb BA. Processing, structure, and properties of carbon fibers. Compos A Appl Sci Manuf 2016;91:262–82. https://doi.org/10.1016/j.compositesa.2016.10.018.
[7] Song YS, Youn JR, Gutowski TG. Life cycle energy analysis of fiber-reinforced composites. Compos A Appl Sci Manuf 2009;40(8):1257–65. https://doi.org/10.1016/j.compositesa.2009.05.020.
[8] Design and Manufacture of Structural Composites. 1st Edition ed: Woodhead Publishing; 2022.
[9] Schmid M, Ramon NG, Dierckx A, Wegman T. accessed 01.07.24 Accelerating Wind Turbine Blade Circularity 2020. https://windeurope.org/wp-content/uploads/files/about-wind/reports/WindEurope-Accelerating-wind-turbine-blade-circularity.pdf,.
[10] Directive 2000/53/EC of the European Parliament and of the Council of 18 September 2000 on end-of life vehicles. https://eur-lex.europa.eu/eli/dir/2000/53/oj, accessed 01.07.24.
[11] Bernatas R, Dagreou S, Despax-Ferreres A, Barasinski A. Recycling of fiber reinforced composites with a focus on thermoplastic composites. Cleaner Eng Technol 2021;5:100272. https://doi.org/10.1016/j.clet.2021.100272.
[12] Krauklis AE, Karl CW, Gagani AI, Jørgensen JK. Composite material recycling technology—state-of-the-art and sustainable development for the 2020s. J Comp Sci 2021;5(1):28. https://doi.org/10.3390/jcs5010028.
[13] Zhang J, Chevali VS, Wang H, Wang C-H. Current status of carbon fibre and carbon fibre composites recycling. Compos B Eng 2020;193:108053. https://doi.org/10.1016/j.compositesb.2020.108053.
[14] Jagadeesh P, Mavinkere Rangappa S, Siengchin S, Puttegowda M, Thiagamani SMK, G. r,, et al. Sustainable recycling technologies for thermoplastic polymers and their composites: A review of the state of the art. Polym Compos 2022;43(9):5831–62. https://doi.org/10.1002/pc.27000.
[15] Pakdel E, Kashi S, Varley R, Wang X. Recent progress in recycling carbon fibre reinforced composites and dry carbon fibre wastes. Resour Conserv Recycl 2021;166:105340. https://doi.org/10.1016/j.resconrec.2020.105340.
[16] Almushaikeh AM, Alaswad SO, Alsuhybani MS, AlOtaibi BM, Alarifi IM, Alqahtani NB, et al. Manufacturing of carbon fiber reinforced thermoplastics and its recovery of carbon fiber: A review. Polym Test 2023;122:108029. https://doi.org/10.1016/j.polymertesting.2023.108029.
[17] Qureshi J. A review of recycling methods for fibre reinforced polymer composites. Sustainability 2022;14(24):16855. https://doi.org/10.3390/su142416855.
[18] Shehab E, Meiirbekov A, Amantayeva A, Tokbolat S. Cost modelling for recycling fiber-reinforced composites: state-of-the-art and future research. Polymers 2023;15(1):150. https://doi.org/10.3390/polym15010150.
[19] Liu Z, Turner TA, Wong KH, Pickering SJ. Development of high performance recycled carbon fibre composites with an advanced hydrodynamic fibre alignment process. J Clean Prod 2021;278:123785. https://doi.org/10.1016/j.jclepro.2020.123785.
[20] Longana ML, Ong N, Yu H, Potter KD. Multiple closed loop recycling of carbon fibre composites with the HiPerDiF (High Performance Discontinuous Fibre) method. Compos Struct 2016;153:271–7. https://doi.org/10.1016/j.compstruct.2016.06.018.
[21] Heider D, Tierney J, Henchir MA, Gargitter V, Yarlagadda S, Jr. JWG, et al. Microstructural Evaluation of Aligned, Short Fiber TUFF Material. SAMPE 2019. Charlotte, NC2019. https://doi.org/10.33599/nasampe/s.19.1609.
[22] Vincent GA, Bruijn TA, Wijskamp S, Rasheed MIA, van Drongelen M, Akkerman R. Characterisation and improvement of the quality of mixing of recycled thermoplastic composites. Compos, Part C: Open Access 2021;4:100108. https://doi.org/10.1016/j.jcomc.2021.100108.
[23] Kiss P, Stadlbauer W, Burgstaller C, Stadler H, Fehringer S, Haeuserer F, et al. In-house recycling of carbon- and glass fibre-reinforced thermoplastic composite laminate waste into high-performance sheet materials. Compos A Appl Sci Manuf 2020;139:106110. https://doi.org/10.1016/j.compositesa.2020.106110.
[24] Soh SL, Ong SK, Nee AYC. Design for disassembly for remanufacturing: Methodology and technology. Procedia CIRP 2014;15:407–12. https://doi.org/10.1016/j.procir.2014.06.053.
[25] Tian X, Liu T, Wang Q, Dilmurat A, Li D, Ziegmann G. Recycling and remanufacturing of 3D printed continuous carbon fiber reinforced PLA composites. J Clean Prod 2017;142:1609–18. https://doi.org/10.1016/j.jclepro.2016.11.139.
[26] Janssen H. Method And Device For Recycling Thermoplastic Fibre - Reinforced Composite Material. Fraunhofer -G esellschaft zur Förderung der angewandten Forschung e.V. , Munich; 2020. US 10,723,043.
[27] Jongebloed P, Schafaschek J, Janssen H, Brecher C. Characterization of recycled thermoplastic unidirectional tapes. 6th International Conference on Thermoplastic Composites. Bremen, Germany2022.
[28] Imbert M, Hahn P, Jung M, Balle F, May M. Mechanical laminae separation at room temperature as a high-quality recycling process for laminated composites. Mater Lett 2022;306:130964. https://doi.org/10.1016/j.matlet.2021.130964.
[29] Grenier R, Imbert M, Hohe J, Balle F, May M. Thermally Assisted Peeling As A High-Quality Disassembly Process For Thermoplastic Tape Wound Composites. 23rd International Conference on Composite Materials. Belfast, UK2023. https://az659834.vo.msecnd.net/eventsairwesteuprod/production-confpartners-public/2e201bc040ae4e468a4929f188e4c1e6, accessed 01.11.24.
[30] Ragupathi B, Bacher MF, Balle F. Separation and reconsolidation of thermoplastic glass fiber composites by power ultrasonics. Resour Conserv Recycl 2023;198:107122. https://doi.org/10.1016/j.resconrec.2023.107122.
[31] Becker M, Imbert M, May M. An inverse model for the peeling-based recovery of unitary layers from laminated structures. AIP Conf Proc 2023;2872(1). https://doi.org/10.1063/5.0163191.
[32] Banea MD, da Silva LFM. Adhesively bonded joints in composite materials: An overview. Proceedings of the Institution of Mechanical Engineers, Part L: Journal of Materials: Design and Applications. 2009;223(1):1-18. https://doi.org/10.1243/14644207jmda219.
[33] von Freeden J, Erb J, Schleifenbaum M. Separating layer recycling strategy for continuous fiber reinforced thermo-sets based on thermally expanding particles. Polym Compos 2022;43(4):1887–99. https://doi.org/10.1002/pc.26505.
[34] Ji X, Matsuo S, Sottos NR, Cahill DG. Anisotropic thermal and electrical conductivities of individual polyacrylonitrile-based carbon fibers. Carbon 2022;197:1–9. https://doi.org/10.1016/j.carbon.2022.06.005.
[35] Längauer M, Brunnthaller F, Zitzenbacher G, Burgstaller C, Hochenauer C. Modeling of the anisotropic thermal conductivity of fabrics embedded in a thermoplastic matrix system. Polym Compos 2021;42(4):2050–60. https://doi.org/10.1002/pc.25958.
[36] Pawlak S, Tokarski M, Ryfa A, Orlande HRB, Adamczyk W. Measurement of the anisotropic thermal conductivity of carbon-fiber/epoxy composites based on laser-induced temperature field: Experimental investigation and numerical analysis. Int Commun Heat Mass Transfer 2022;139:106401. https://doi.org/10.1016/j.icheatmasstransfer.2022.106401.